Pergamon

Int. J. Solids Structures Vol. 33, No. 3, pp. 419–432, 1996

0020–7683/96 $9.50 + .00

0020–7683(95)00048–8

FINITE ELEMENT MODELING OF FREQUENCY-DEPENDENT AND TEMPERATURE-DEPENDENT DYNAMIC BEHAVIOR OF VISCOELASTIC MATERIALS IN SIMPLE SHEAR

GEORGE A. LESIEUTRE and KIRAN GOVINDSWAMY
Department of Aerospace Engineering, 233 Hammond Building, The Pennsylvania State University, University Park, PA 16802, U.S.A.

(*Received* 17 *March* 1994; *in revised form* 22 *February* 1995)

Abstract—Material dynamic mechanical behavior can depend strongly on frequency and temperature. This dependence is especially significant for elastomers and polymers, such as those used in bearings and damping treatments. Previous research has yielded a time-domain model of linear viscoelastic material and structural behavior that captures characteristic frequency-dependent behavior; continuing research has addressed the accommodation of temperature dependence as well. The resulting approach is based on the notion of time–temperature superposition for thermorheologically-simple materials. In such materials, temperature effects are experienced primarily through a temperature-dependent factor multiplying the time scale. The phenomenon of "thermal runaway", observed in some tests of helicopter elastomeric dampers, motivates a numerical example of forced vibration of a $40 \times 16 \times 5$ mm elastomeric test specimen in simple shear. For forcing at 1500 N and 4 Hz, and the temperature on one face held constant, the temperature at the thermally free face increases by about 3 K. For forcing at 3000 N, the temperature rapidly increases more than 35 K, and displacement amplitudes increase by more than a factor of 4. The coupled-field finite element simulation evidently captures the key features of observed material response, including a rapidly increasing rate of temperature change and an accompanying stiffness reduction.

INTRODUCTION

Vibration damping is essential to the attainment of performance goals for engineered systems that can exhibit significant structural dynamic response. Passive structural damping can be increased most predictably through the use of materials with known damping properties. Because of the potential for practical payoffs, some research efforts have pursued the development of structural materials (typically composites) with increased damping properties. However, the most common method used today to increase structural damping involves the use of non-structural materials, typically high-damping viscoelastic polymers or elastomers (Nashif *et al.*, 1985).

The mechanical properties of these "damping materials" are often sensitive to frequency, temperature, type of deformation (i.e. shear or dilation) and sometimes amplitude. To ensure design adequacy, performance is usually evaluated analytically at a few specific temperatures that span the expected operating range of the system of interest. Material properties appropriate to each single temperature of interest are used in these analyses. A time-domain modeling approach capable of including temperature effects directly would be useful, especially in applications where dissipative self-heating is important, such as in helicopter lead-lag dampers (Hausmann and Gergely, 1992).

Damping models currently available in commercial finite element software (e.g. viscous damping, proportional damping, hysteretic or structural damping and viscous modal damping) are generally not physically motivated. These models do not explicitly preserve the fundamental temperature-dependent or frequency-dependent behavior of real materials, and each suffers in practice from one difficulty or another. Although better accuracy is potentially available through the use of material models like general viscoelasticity, such models are not widely used in engineering applications.

The most common approach to analysis of damping designs using viscoelastic polymers is perhaps the modal strain energy (MSE) method (Rogers *et al.*, 1981). In this approach, a modal analysis of an elastic structure is performed using material properties appropriate to one specific temperature and frequency. Effective modal damping ratios are found for each normal vibration mode as a weighted sum of the damping of the constituent materials, where the weighting factor is the fraction of total modal strain energy stored in each. When several modal damping ratios are to be determined, use of the MSE method involves an iterative process. Because of the frequency dependence of material properties, suitable definition of each mode requires the use of properties appropriate to a (small) frequency range containing that modal frequency.

Dynamic models based on the use of the typical MSE method and "modal damping" can have several weaknesses: iteration is required to determine the modal damping for each vibration mode in the frequency range of interest, the resulting modes are not orthogonal in any familiar sense because of the non-uniqueness of the stiffness matrix, the relative phase of vibration at various points on a structure is neglected and modes that are closely-spaced in frequency may be predicted poorly. In addition, the effects of dissipative self-heating on material behavior are usually neglected or, at best, considered only crudely.

The development of modeling approaches that capture the essential temperature dependence and frequency dependence of viscoelastic material properties, and that are compatible with current structural finite element analysis techniques, is an area of ongoing research.

Considerable recent effort has addressed the frequency dependence of material behavior. The augmenting thermodynamic fields modeling method (Lesieutre and Mingori, 1990) is one such time-domain continuum model of material damping that preserves the characteristic frequency-dependent damping and modulus of real materials—a physically-motivated model compatible with current finite element structural analysis methods. In its initial development, this method introduced single augmenting fields to model the behavior of materials and structures with light damping. In subsequent work, the ability to model high-damping materials with relatively weak frequency dependence using multiple augmenting fields was developed (Lesieutre, 1992). However, this early work was limited to effectively one-dimensional stress states, such as those present in idealized (single-modulus) structural bar and beam members.

Recent research extended the initial work to the general case of three-dimensional stress states, introducing "anelastic displacement fields" (ADFs), which are special kinds of augmenting fields (Lesieutre and Bianchini, 1994). Instead of addressing physical damping mechanisms directly, as in the earlier approach, their effects on the displacement field are considered. In the ADF approach, the total displacement field is comprised of two parts, an elastic part and an anelastic part. An approach for determining needed material properties (model parameters) from available data was also developed. The general capabilities of the approach have been demonstrated through modal analyses, stress–strain hysteresis loops and frequency response analyses. The key practical benefit of the ADF approach is that it leads to straightforward development of time-domain viscoelastic finite elements.

While dissatisfaction with available techniques has motivated several alternative lines of research, two are most closely related to the ADF model. Both of these, the GHM model (McTavish and Hughes, 1993; Golla and Hughes, 1985) and Yiu's model (Yiu, 1993), lead to viscoelastic finite elements and use additional coordinates to model more accurately material behavior. The ADF method is primarily distinguished from these in that it is a direct time-domain formulation, not transform-based, and it yields finite elements using conventional methods (i.e. the method of weighted residuals). In addition, the "dissipation coordinates" of the GHM method are internal to individual elements, while the physically-significant ADFs of ADF are continuous from element to element, reflecting its basis as a field theory. The "internal unobservable degrees of freedom" of Yiu's model are introduced as nodal variables using an analogy with a generalized lumped-parameter Maxwell model.

As it was intentionally developed with second-order dynamics, the GHM method is quite compatible with current structural analysis methods, and has proven to be useful in practice; both the ADF and Yiu's models may also be readily expressed in second-order form. In its current state of development, Yiu's model assumes a single loss factor for all

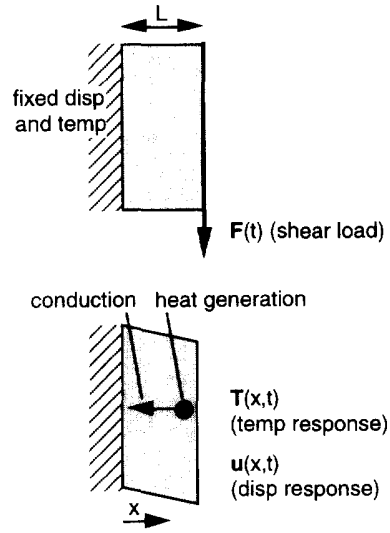

Fig. 1. Configuration considered.

material moduli (e.g. shear and bulk for an isotropic material). In many respects, however, finite element models that result from the use of the GHM method and especially Yiu's method are quite similar to ADF models.

All three of these approaches have advantages over the MSE method in that they yield linear time-domain finite element models, the frequency-dependent elastic and dissipative aspects of structural behavior are represented in fixed (not frequency-dependent) system matrices, modal damping is calculated concurrently with modal frequency without iteration, the resulting complex modes more accurately reflect the relative phase of vibration at various points and modal orthogonality is preserved.

The interested reader is referred to the references for the details of the various models discussed. None of these approaches have explicitly addressed the essential temperature dependence of material behavior.

INCORPORATION OF TEMPERATURE DEPENDENCE IN THE ADF MODEL

Recent research has addressed the incorporation of characteristic temperature-dependent mechanical behavior in the ADF model. This advance is founded on the notion of time–temperature superposition for thermorheologically-simple materials (cf., Ferry, 1980). Motivated by a helicopter damper application, a simple structure serves as the focus for theoretical development and numerical study. Figure 1 shows the general specimen and loading configuration considered. This configuration is representative of elastomer characterization experiments.

In such an experiment, a uniform elastomeric element is subjected to harmonic forced vibration in simple shear; because of the viscoelastic nature of the material, some of the energy of vibration is converted to heat. This distributed heat input changes the local temperature of the material. Thermal conduction transfers some of this heat to the base (environment), which is maintained at a fixed temperature. Local temperature changes affect the rate at which the local anelastic displacement relaxes—higher temperatures result in faster relaxation and lower apparent stiffness. Lower stiffness results in larger displacements and possibly higher energy dissipation. If vibration energy is converted to heat at a rate faster than the heat is conducted away, the local temperature increases. If the temperature change is small enough, the material properties may not change appreciably, and the rate of temperature increase slows monotonically as the specimen approaches a kind of thermal equilibrium state. If the rate of temperature increase itself increases as the

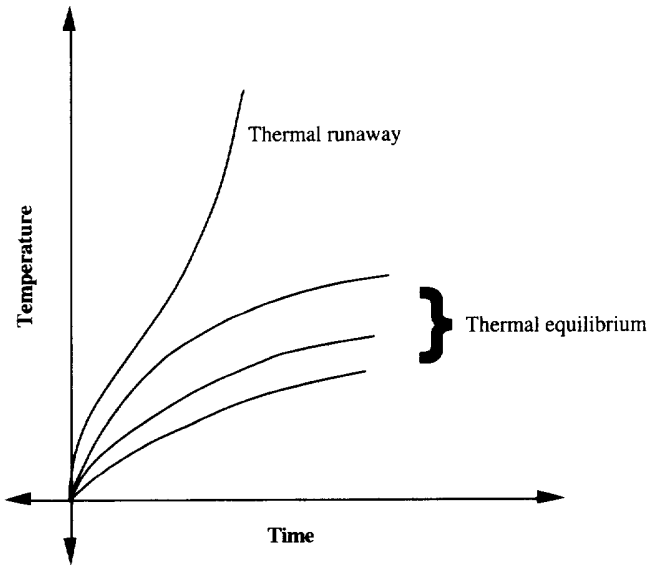

Fig. 2. Thermal runaway.

result of changing material properties, as illustrated in Fig. 2 [adapted from Hausmann and Gergely (1992)], a phenomenon called "thermal runaway" is possible. Depending on the magnitude of the temperature increase, the specimen may approach an alternative thermal equilibrium state, or chemical reactions may change the fundamental nature of the material. This general phenomenon has reportedly been observed in tests of helicopter lead-lag dampers (Hausmann and Gergely, 1992), although the details of the materials and test conditions were not reported.

The following sections describe key steps in the development of a model which addresses these physical processes. To provide a point of departure for the development, the first section summarizes the theory for the one-dimensional ADF model without temperature dependence, the subsequent section develops the one-dimensional ADF model with temperature dependence, and the next provides a numerical example of the use of this model.

ONE-DIMENSIONAL ADF MODEL WITHOUT TEMPERATURE DEPENDENCE

The ADF model of linear viscoelasticity (Lesieutre and Bianchini, 1994) is based on a decomposition of the total displacement field into two parts, one elastic, the other anelastic. The anelastic displacement field is used to describe that part of the strain that is not instantaneously proportional to stress. General coupled material constitutive equations for: (1) the total; and (2) the anelastic stresses are developed in terms of the total and anelastic strains, and may be specialized to the case of, for example, isotropic materials.

A key feature of the model is the absence of explicit time dependence in the material constitutive equations. Apparent time-dependent or frequency-dependent behavior is described instead by two sets of differential equations that govern: (1) the motion of mass particles; and (2) the relaxation of the anelastic displacement field. These coupled governing equations are developed in a parallel fashion, both involving the divergence of appropriate stress tensors. Boundary conditions are also treated: the anelastic displacement field is effectively an internal field, as it is driven exclusively through coupling to the total displacement, and cannot be directly affected by external applied loads. ADF model parameters may be readily developed from available complex modulus data.

Material constitutive equations

In the present one-dimensional problem of simple shear, $u(x, t)$ is the total transverse displacement field, while $u^A(x, t)$ is the anelastic part of the displacement field. For clarity,

a single ADF is used to model the anelastic behavior. (Multiple ADFs may be used to model the behavior of materials that exhibit relatively weak frequency dependence.) The constitutive equations for the shear stress and the anelastic shear stress are (Lesieutre *et al.*, 1995):

$$\sigma = G_u(u' - u'^A) \quad \text{(stress)} \tag{1a}$$

$$\sigma^A = G_u(u' - cu'^A) \quad \text{(anelastic stress).} \tag{1b}$$

Note that these are "equations of state" in a thermodynamic sense, in that there is no explicit time dependence. G_u is the unrelaxed or high-frequency dynamic shear modulus of the material and c is a coupling property. The quantity cG_u could also be considered an anelastic shear modulus, G^A.

Governing differential equations

The "equation of motion" governing the dynamics of mass particles in this one-dimensional elastomeric specimen is:

$$\rho\ddot{u} - G_u u'' + G_u u''^A = p(x, t), \tag{2}$$

where $p(x, t)$ is a distributed shear load. The boundary conditions are the familiar ones involving the total displacement or stress at each end of the specimen.

The "relaxation equation" governing the time evolution of the specimen anelastic displacement field $u^A(x, t)$ is found using a fundamental assumption of non-equilibrium thermodynamics, namely that the rate of change of the state variable describing an irreversible process is proportional to the corresponding conjugate quantity. Alternatively, the quantity σ^A may be interpreted as a "thermodynamic force" driving an anelastic strain component, ε^A, towards an equilibrium value: σ^A is zero when ε^A takes on its equilibrium value. Then, the time rate of change of ε^A is proportional to the difference between the value of ε^A and its instantaneous equilibrium value, $\bar{\varepsilon}^A$. The constant of proportionality is the inverse of the relaxation time at constant strain, Ω.

The "relaxation equation" governing the time evolution of the anelastic displacement field is given by:

$$\frac{cG_u}{\Omega}\dot{u}'^A - G_u u'' + cG_u u''^A = 0. \tag{3}$$

Note that this equation is first-order in time.

The thermal behavior of the (uniform) specimen is described by:

$$c_v\dot{T} - kT'' = r(x, t), \tag{4}$$

where T is the temperature, c_v is the heat capacity at constant strain, k is the thermal conductivity and $r(x, t)$ is the distributed heat source strength. This heat source strength is due to internal energy conversion ("dissipation") and is given by:

$$r(x, t) = \frac{cG_u}{\Omega}(\dot{u}'^A)^2. \tag{5}$$

Note that this is quadratic in the anelastic strain rate.

A classical mechanical analogy

In that a single-ADF model may be considered to be a continuum version of the standard anelastic solid, a physical interpretation of some of the quantities involved in the one-dimensional ADF model may be advanced in terms of a classical mechanical analogy

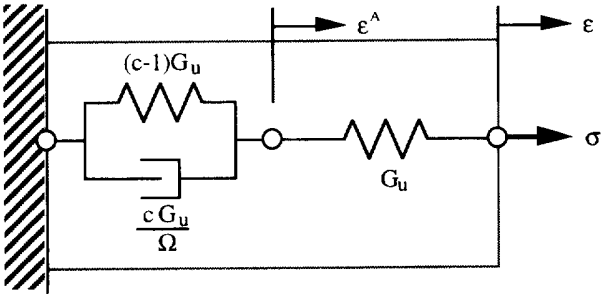

Fig. 3. Mechanical analogy for single ADF model.

(Lesieutre *et al.*, 1995). Consider the lumped-parameter system shown in Fig. 3, comprised of a parallel spring-dashpot unit in series with a spring unit. The displacement and force at the right side correspond to the total strain and stress, respectively, while the internal displacement corresponds to the anelastic strain. The anelastic stress is analogous to the force in the dashpot unit. The energy dissipated in the dashpot is quadratic in the anelastic strain rate.

The property G_u may be considered the high-frequency stiffness, while the quantity $G_u(c-1)/c$ may be considered the low-frequency stiffness. The parameter Ω determines the frequency near which the stiffness transition occurs and peak damping is observed.

ONE-DIMENSIONAL ADF MODEL WITH TEMPERATURE DEPENDENCE

Temperature dependence was not considered in the development of the preceding equations. The key step in the inclusion of temperature dependence is to consider the elastomer to be a thermorheologically-simple material. In such materials, temperature effects are experienced primarily through a temperature-dependent factor multiplying the time scale (Brinson and Knauss, 1991). This quantity, $\alpha_T(T)$, is called the time–temperature shift factor.

For a thermorheologically-simple material, time and temperature are related through a quantity called reduced time, t_R (Rogers and Fowler, 1991). This relationship is most conveniently defined in differential form as (Moreland and Lee, 1960):

$$\alpha_T \, dt_R = dt. \tag{6a}$$

Use of the differential relationship is essential when the system of interest is non-uniform in temperature. Alternatively, the corresponding time rates of change are related by:

$$\frac{d}{dt_R} = \alpha_T \frac{d}{dt}. \tag{6b}$$

Note that because α_T generally decreases with increasing temperature, eqns (6a,b) may be interpreted physically as follows: an event that occurs in a fixed increment of reduced time (at a reference temperature) occurs in an actual time that decreases with increasing temperature [eqn 6(a)]; or actual relaxation rates increase with increasing temperature [eqn (6b)].

Now, if the material properties G_u, c and Ω are determined from data expressed relative to "reduced frequency" [related to reduced time; Soovere and Drake (1985)] spanning the operational temperature and frequency range of interest, they may be regarded as constant parameters. (Note that multiple ADFs may be needed to represent adequately the data over a broad operating range.) The material constitutive equations [eqns (1a,b)] and the equation of motion [eqn (2)] are thus unchanged from those presented in the preceding work. However, the relaxation of the anelastic displacement field proceeds at a higher rate at higher temperatures. Since material properties have been determined with respect to

reduced frequency in the present development, the time derivative in the relaxation equation previously presented [eqn (3)] is understood to be with respect to reduced time (as is the relaxation parameter, Ω).

$$\frac{cG_u}{\Omega}\frac{\hat{c}}{\hat{c}t_R}(u''^A) - G_u u'' + cG_u u''^A = 0. \tag{7}$$

Using the time–temperature shift factor from eqn (6b), this relaxation equation may then be expressed in terms of actual time as:

$$\alpha_T \frac{cG_u}{\Omega}\dot{u}''^A - G_u u'' + cG_u u''^A = 0. \tag{8}$$

This may be further simplified through the introduction of a new parameter, Ω_T, that effectively describes how the actual relaxation rate changes with temperature. It is defined in terms of the relaxation parameter with respect to reduced time and the time–temperature shift factor as:

$$\Omega_T = \frac{\Omega}{\alpha_T}. \tag{9}$$

As noted, the general effect of increasing temperature is to decrease α_T, thereby increasing the relaxation rate. Using this new parameter, the relaxation equation may be expressed in essentially the same form as eqn (3), changed only by the presence of a temperature-dependent relaxation parameter, Ω_T.

$$\frac{cG_u}{\Omega_T}\dot{u}''^A - G_u u'' + cG_u u''^A = 0.$$

The heat source strength [eqn (5)] may then be expressed as:

$$r(x,t) = \alpha_T \frac{cG_u}{\Omega}(\dot{u}'^A)^2 = \frac{cG_u}{\Omega_T}(\dot{u}'^A)^2. \tag{10}$$

Time–temperature shift factor

A classical Arrhenius relationship for the time–temperature shift factor is used in what follows for simplicity. Such a relationship has the following form:

$$\alpha_T(T) = e^{a[(1/T) - (1/T_{ref})]}, \tag{11}$$

where a and T_{ref} are material parameters. Time–temperature shift factors for real materials are often determined empirically and usually take forms other than the Arrhenius form. An important such practical form is the "WLF equation" (Ferry, 1980).

NUMERICAL EXAMPLE AND RESULTS

The forced simple shear vibration problem described was addressed numerically using the one-dimensional ADF theory with temperature dependence. A small number of finite elements, typically four to 10, were used to explore the general ability of the subject method to capture essential features of the mechanical and thermal response.

The specimen geometry, material properties and load amplitude and frequency used in the numerical examples were selected to be representative of elastomer characterization tests. The specimen was assumed to have a finite cross-section with thermally insulated sides, so that little heat could be lost to the environment on the sides. In addition, the specimen had a fixed temperature thermal boundary on one face in order to allow for heat

Table 1. Parameters used in numerical examples

Thickness	L	0.00508 m
Area	A	6.45×10^{-4} m^2 (0.0159 × 0.0406 m)
Density	ρ	926.8 kg m^{-3}
Shear modulus (high frequency)	G_u	10.5×10^6 N m^{-2}
Coupling parameter	c	1.5
Relaxation parameter	Ω	25.13 s^{-1}
Modulus (low frequency)	G_1	3.5×10^6 N m^{-2}
Max loss factor	η_{max}	0.577
Temperature shift parameter	a	9000 K
Reference temperature	T_{ref}	300 K
Thermal conductivity (untreated)	k	5.00 W m^{-1} K^{-1} (0.155 W m^{-1} K^{-1})
Heat capacity	c_v	1.65×10^6 J m^{-3} K^{-1}
Specimen base temperature	T_0	285 K
Force amplitudes	F	1500, 3000 N
Force frequency	f	4.0 Hz
Integration time step	Δt	0.01 s

flow to the environment, approximating the effect of attachment to a large thermal mass (or heat sink) having considerably higher thermal conductivity than the material specimen itself.

In order to limit peak temperature excursions and to speed attainment of thermal equilibrium, specimen thermal conductivity was increased by about a factor of 30 over that of an untreated elastomer; the effect is similar to that of using internal metal "shims", which is done in practice for several reasons. Dependence of thermal conductivity and heat capacity on temperature was neglected in the analysis. Table 1 summarizes important parameters used in the numerical simulation.

The governing differential equations were discretized using the method of weighted residuals. Figure 4 illustrates the one-dimensional shear finite element used; it has three nodal variables at each end, each of which is interpolated linearly across the element. The nodal variables are: u, total displacement; u^A, anelastic displacement; and T, temperature.

The resulting discretized elemental equations have the following general state-space form:

$$\begin{bmatrix} m & 0 & 0 & 0 \\ 0 & 1 & 0 & 0 \\ 0 & 0 & \alpha_T \dfrac{c}{\Omega} k & 0 \\ 0 & 0 & 0 & C \end{bmatrix} \begin{Bmatrix} \ddot{u} \\ \dot{u} \\ \dot{u}^A \\ \dot{T} \end{Bmatrix} + \begin{bmatrix} 0 & k & -k & 0 \\ -1 & 0 & 0 & 0 \\ 0 & -k & ck & 0 \\ 0 & 0 & 0 & K \end{bmatrix} \begin{Bmatrix} \dot{u} \\ u \\ u^A \\ T \end{Bmatrix} = \begin{Bmatrix} F \\ 0 \\ 0 \\ R \end{Bmatrix}, \quad (12)$$

where individual sub-matrices involve terms like:

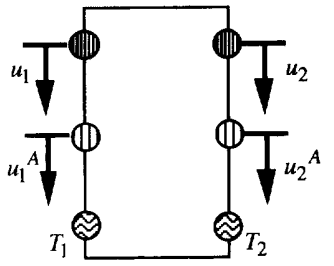

Fig. 4. Single ADF finite element for simple shear with changing temperature.

$$m = \rho A L_{el} \qquad \text{"mass"}$$

$$k = G_u A / L_{el} \qquad \text{"stiffness"}$$

$$C = c_v A L_{el} \qquad \text{"heat capacity"}$$

$$K = kA / L_{el} \qquad \text{"thermal conductivity"}$$

$$R = (\alpha_T ck/\Omega)(\dot{u}^A)^2 = (ck/\Omega_T)(\dot{u}^A)^2 \qquad \text{"heat generation".}$$

The elemental equations of evolution may also be expressed in second-order form as:

$$[\mathbf{M}]\{\ddot{\mathbf{x}}\} + [\mathbf{C}]\{\dot{\mathbf{x}}\} + [\mathbf{K}]\{\mathbf{x}\} = \{\mathbf{f}\}, \tag{13a}$$

where the individual matrices have the following general structure:

$$\begin{bmatrix} m & 0 & 0 \\ 0 & 0 & 0 \\ 0 & 0 & 0 \end{bmatrix} \begin{Bmatrix} \ddot{u} \\ \ddot{u}^A \\ \ddot{T} \end{Bmatrix} + \begin{bmatrix} 0 & 0 & 0 \\ 0 & \alpha_T \dfrac{c}{\Omega} k & 0 \\ 0 & (\ )\dot{u}^A & C \end{bmatrix} \begin{Bmatrix} \dot{u} \\ \dot{u}^A \\ \dot{T} \end{Bmatrix} + \begin{bmatrix} k & -k & 0 \\ -k & ck & 0 \\ 0 & 0 & K \end{bmatrix} \begin{Bmatrix} u \\ u^A \\ T \end{Bmatrix} = \begin{Bmatrix} F \\ 0 \\ 0 \end{Bmatrix}. \tag{13b}$$

Note that the heat generation terms, R, that "force" the thermal response in eqn (12), have been moved to the left-hand side. The following equations provide additional details of the individual matrices and nodal vectors:

$$\{\mathbf{x}\} = \begin{Bmatrix} u_1 \\ u_1^A \\ T_1 \\ u_2 \\ u_2^A \\ T_2 \end{Bmatrix} \tag{14a}$$

$$[\mathbf{M}] = \begin{bmatrix} m/3 & 0 & 0 & m/6 & 0 & 0 \\ 0 & 0 & 0 & 0 & 0 & 0 \\ 0 & 0 & 0 & 0 & 0 & 0 \\ m/6 & 0 & 0 & m/3 & 0 & 0 \\ 0 & 0 & 0 & 0 & 0 & 0 \\ 0 & 0 & 0 & 0 & 0 & 0 \end{bmatrix} \tag{14b}$$

$$[\mathbf{C}] = \begin{bmatrix} 0 & 0 & 0 & 0 & 0 & 0 \\ 0 & \dfrac{ck}{\Omega_T} & 0 & 0 & -\dfrac{ck}{\Omega_T} & 0 \\ 0 & \left(\dfrac{ck}{\Omega_T}\left(\dfrac{\dot{u}_2^A - \dot{u}_1^A}{2}\right)\right) & \dfrac{C}{3} & 0 & -\left(\dfrac{ck}{\Omega_T}\left(\dfrac{\dot{u}_2^A - \dot{u}_1^A}{2}\right)\right) & \dfrac{C}{6} \\ 0 & 0 & 0 & 0 & 0 & 0 \\ 0 & -\dfrac{ck}{\Omega_T} & 0 & 0 & \dfrac{ck}{\Omega_T} & 0 \\ 0 & \left(\dfrac{ck}{\Omega_T}\left(\dfrac{\dot{u}_2^A - \dot{u}_1^A}{2}\right)\right) & \dfrac{C}{6} & 0 & -\left(\dfrac{ck}{\Omega_T}\left(\dfrac{\dot{u}_2^A - \dot{u}_1^A}{2}\right)\right) & \dfrac{C}{3} \end{bmatrix} \tag{14c}$$

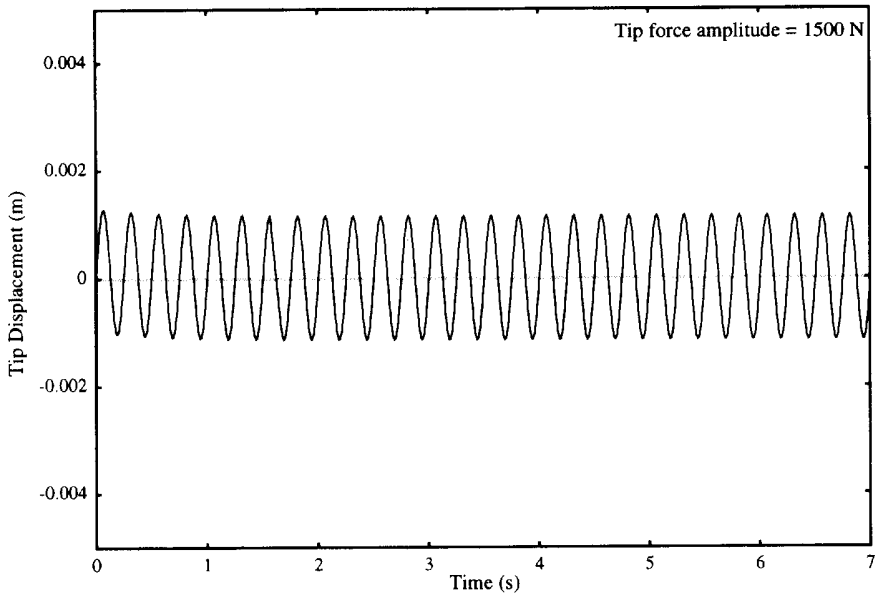

Fig. 5. Tip displacement–time history (1500 N).

$$[\mathbf{K}] = \begin{bmatrix} k & -k & 0 & -k & k & 0 \\ -k & ck & 0 & k & -ck & 0 \\ 0 & 0 & K & 0 & 0 & -K \\ -k & k & 0 & k & -k & 0 \\ k & -ck & 0 & -k & ck & 0 \\ 0 & 0 & -K & 0 & 0 & K \end{bmatrix} \tag{14d}$$

$$\{\mathbf{f}\} = \begin{Bmatrix} f_1(t) \\ 0 \\ 0 \\ f_2(t) \\ 0 \\ 0 \end{Bmatrix}. \tag{14e}$$

The discretized equations were actually solved in second-order form [eqns (13a,b)] using the Newmark single-step integration scheme (Bathe, 1982).

Placing the heat generation terms on the left-hand side of eqns (13a,b) results in a non-symmetric system "damping" matrix. Also note that all of the problem non-linearities are included in this damping matrix. These non-linearities include terms multiplied by α_T, which is a function of the (changing) temperature, as well as the heat generation terms, which are quadratic in the anelastic displacement rates.

To accommodate these non-linearities, an iterative solution scheme was employed. Values of the nodal quantities and their first time derivatives from the end of the previous time step were used to obtain an approximate damping matrix at the beginning of each new time step. Subsequent solutions at the current time step were used to adjust iteratively the damping matrix until the nodal quantities converged to within 1%. This process was repeated at every time step.

The governing matrix equations were integrated forward in time. The specimen was initially motionless, at a constant temperature. At time $t = 0$, harmonic forcing was begun. Nodal displacements and temperatures were determined as functions of time.

Figures 5–8 show typical response results for a relatively low force level of 1500 N. As shown in Fig. 5, the tip displacement magnitude is stable over time following a small initial

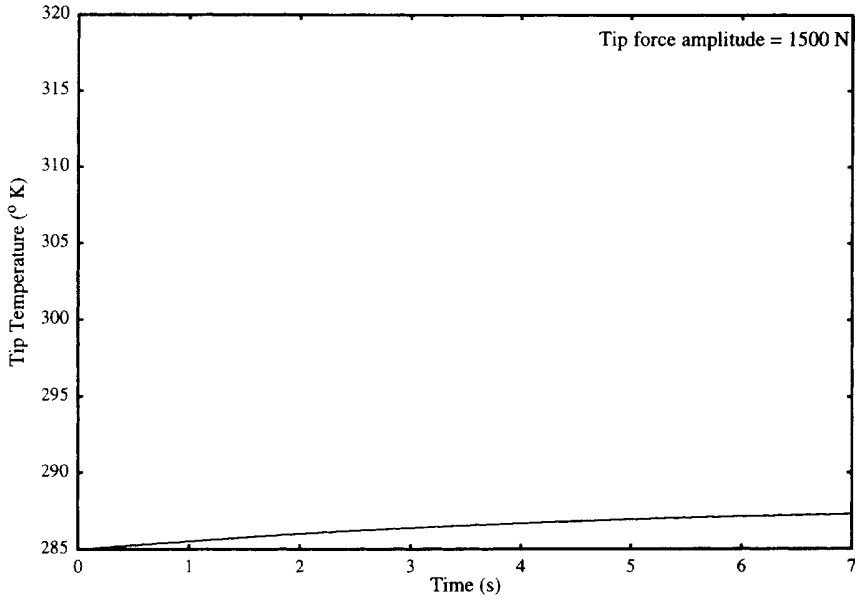

Fig. 6. Tip temperature–time history (1500 N).

transient; the peak displacements correspond to roughly 20% strain. The temperature response shown in Fig. 6 gradually approaches an equilibrium value just a few degrees above that of the base. At this equilibrium temperature, the heat input to the specimen due to material dissipation is balanced by the heat flow out due to thermal conduction. Figure 7 shows the temperature distribution through the thickness of the specimen at $t = 10$ s. As expected, the temperatures decrease from the insulated free face to the cooled base. Figure 8 shows the tip force–displacement trajectory ("hysteresis loops"). Again, this indicates stable specimen response, as the trajectories converge to a single closed curve.

Figures 9–12 show corresponding results for a doubled force level of 3000 N. In this case, the displacement response amplitude shown in Fig. 9 is nearly constant for a period of time, then increases rapidly as the specimen temperature increases; the peak displacements correspond to roughly 100% shear strain. The temperature shown in Fig. 10 increases linearly over the initial period, then increases more rapidly. This has the characteristics of

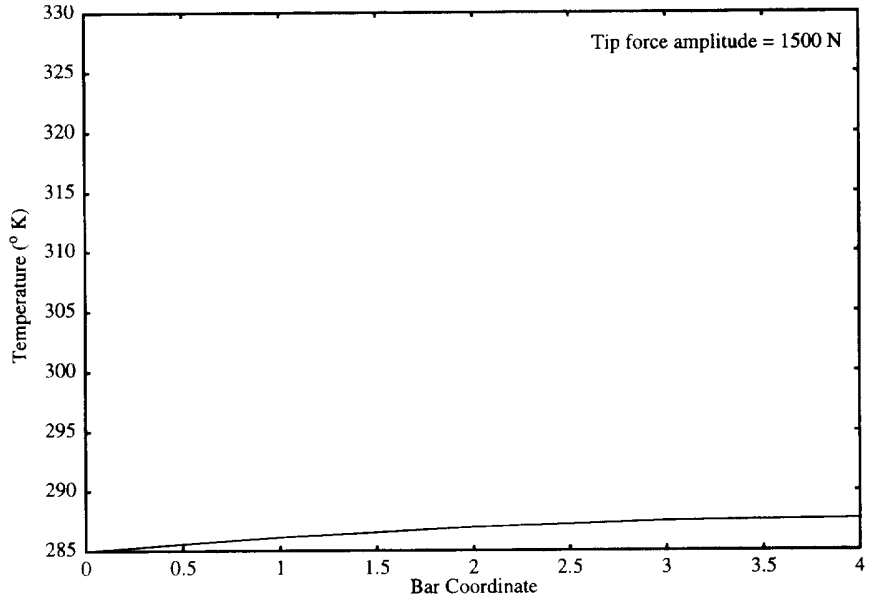

Fig. 7. Nodal temperatures (1500 N; $t = 10$ s).

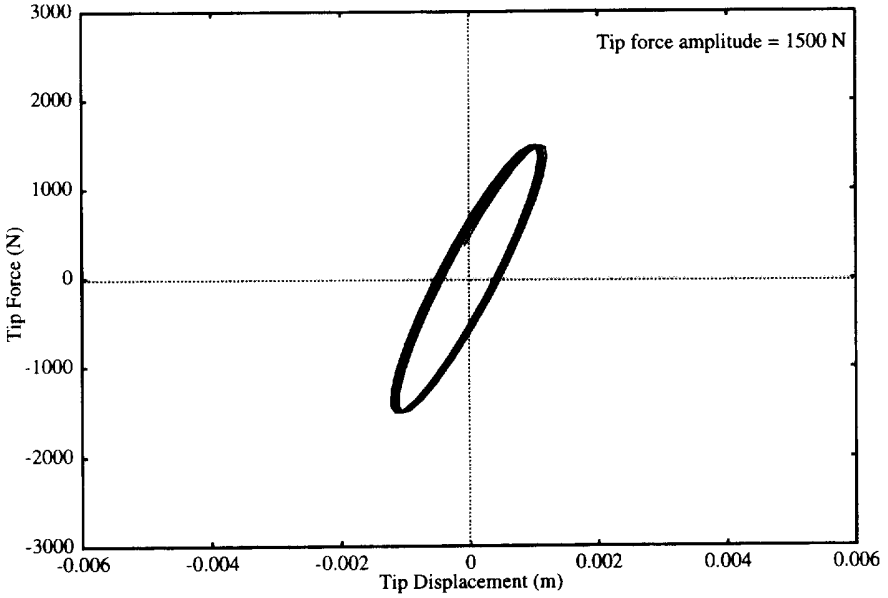

Fig. 8. Hysteresis loops (1500 N).

the "thermal runaway" behavior described previously. (Although not clearly shown in the figure, the temperature does approach a higher equilibrium temperature.) Figure 11 shows the temperature distribution through the thickness of the specimen at $t = 10$ s. The temperature change at the tip is more than an order of magnitude higher than that associated with the lower force level. Figure 12 shows the tip force–displacement trajectory for the higher force case. The changes in slopes and shapes of these trajectories show a marked transition from stiff, lossy behavior to softer, more lossy behavior.

These results appear to indicate the potential of the present approach to accommodate both the temperature-dependent and frequency-dependent behavior of thermo-rheologically-simple viscoelastic materials. This potential will continue to be explored in the future through more complex numerical examples and through laboratory study.

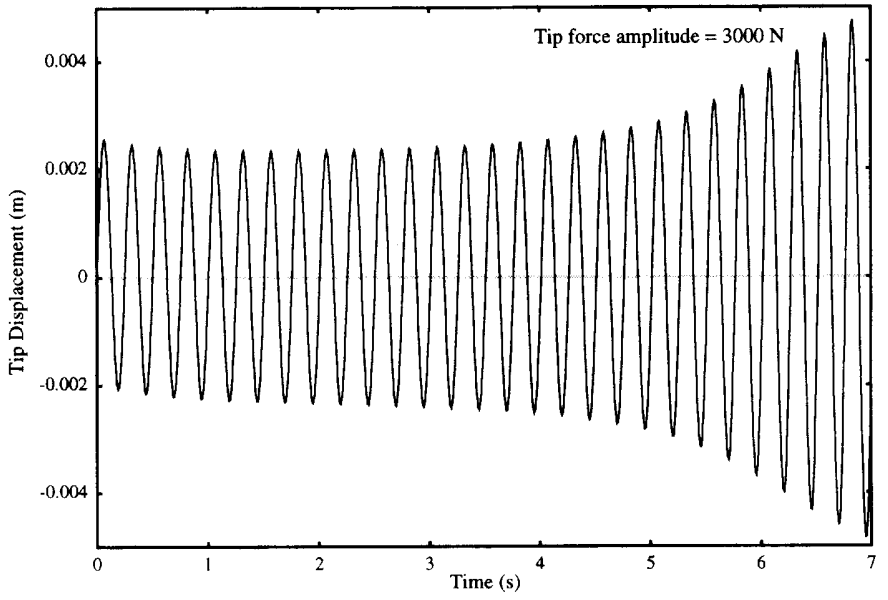

Fig. 9. Tip displacement–time history (3000 N).

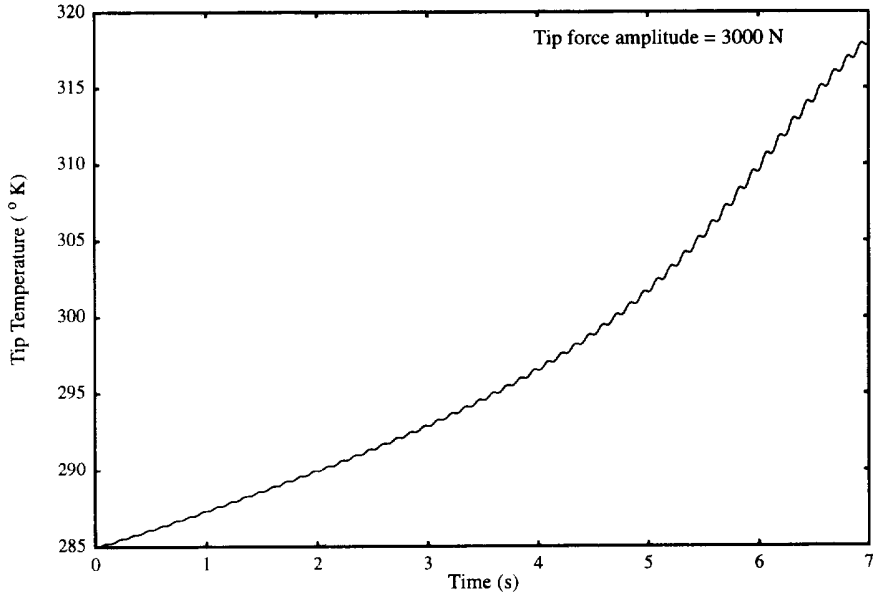

Fig. 10. Tip temperature–time history (3000 N).

SUMMARY

A physically-motivated method for modeling the dynamic behavior of viscoelastic materials and structures continues to be developed. This method, focused initially on capturing the essential frequency-dependent behavior of viscoelastic materials, has been extended to address characteristic temperature dependence as well. This extension is based on the assumption of thermorheologically-simple material behavior. The approach has been illustrated through a numerical example, and appears to capture successfully some of the features of the observed phenomenon of "thermal runaway".

These results suggest direction for the continued development of a general three-dimensional approach. Such an approach would be suitable for describing thermo-rheologically-simple viscoelastic behavior under complex states of stress. Anticipated aerospace applications of this approach might include elastomeric bearings and dampers,

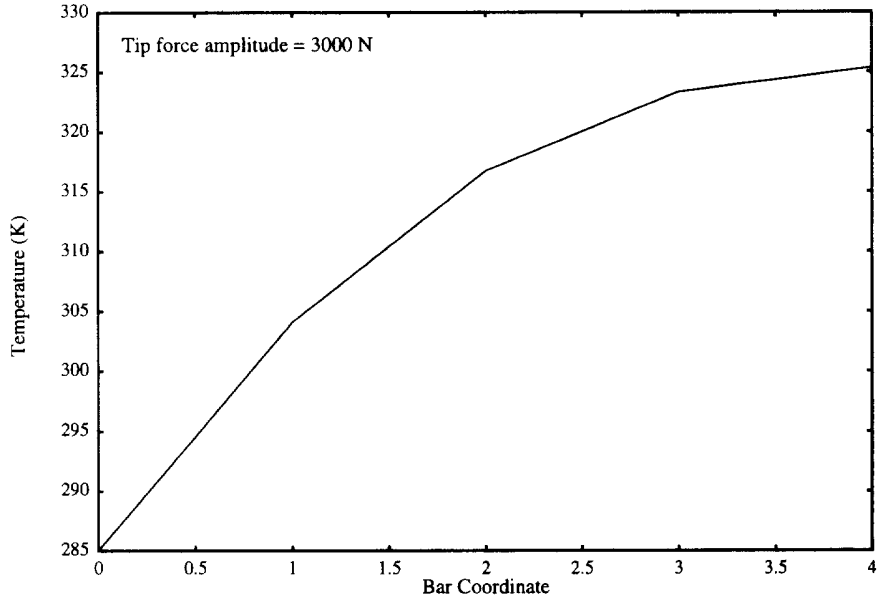

Fig. 11. Nodal temperatures (3000 N; t = 10 s).

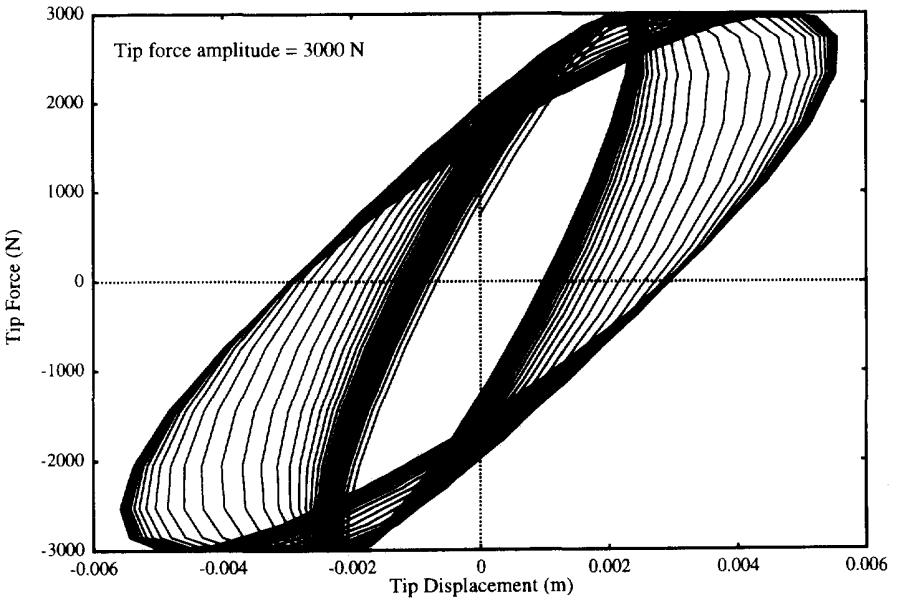

Fig. 12. Hysteresis loops (3000 N).

vibration damping treatments, solid propellant rocket motors, non-destructive evaluation of composite structures and statistical energy analysis of structural acoustics.

Acknowledgements—The authors gratefully acknowledge the Centro Italiano Ricerche Aerospaziali for financial support and Dr Edward C. Smith of Penn State University for suggesting the elastomeric damper problem that motivated this work.

REFERENCES

Bathe, K. J. (1982). *Finite Element Procedure in Engineering Analysis*. Prentice Hall, Englewood Cliffs, New Jersey.

Brinson, L. C. and Knauss, W. G. (1991). Thermorheologically-complex behavior of multi-phase viscoelastic materials. *J. Mech. Phys. Solids* **39,** 859–880.

Ferry, J. D. (1980). *Viscoelastic Properties of Polymers*, 3rd edn. John Wiley, New York.

Golla, D. F. and Hughes, P. C. (1985). Dynamics of viscoelastic structures—a time-domain, finite element formulation. *J. Appl. Mech.* **52,** 897–906.

Hausmann, G. and Gergely, P. (1992). Approximate methods for thermoviscoelastic characterization and analysis of elastomeric lead-lag dampers. *Proceedings of the 18th European Rotorcraft Forum*, Avignon, France, 15–18 September.

Lesieutre, G. A. (1992). Finite elements for dynamic modeling of uniaxial rods with frequency dependent material properties. *Int. J. Solids Structures* **29,** 1567–1579.

Lesieutre, G. A. and Bianchini, E. B. (1994). Time-domain modeling of 3-D continuum viscoelasticity using anelastic displacement fields. *J. Vibr. Acoust.* **117.** In press.

Lesieutre, G. A. and Mingori, D. L. (1990). Finite element modeling of frequency-dependent material damping using augmenting thermodynamic fields. *J. Guidance Control Dynam.* **13,** 1040–1050.

Lesieutre, G. A., Bianchini, E. and Maiani, A. (1995). The use of anelastic displacement fields in finite element modeling of viscoelastic structures. *J. Guidance, Control Dynam.* In press.

McTavish, D. J. and Hughes, P. C. (1993). Modeling of linear viscoelastic space structures. *J. Vibr. Acoust.* **115,** 103–113.

Moreland, L. W. and Lee, E. H (1960). Stress analysis for linear viscoelastic materials with temperature variation. *Trans. Soc. Rheology* **IV,** 233–263.

Nashif, A. D., Jones, D. I. G. and Henderson, J. P. (1985). *Vibration Damping*. John Wiley, New York.

Rogers, L. C. and Fowler, B. (1991). Modelling temperature shift and complex modulus data thru real-imaginary relationships and wicket plots. *Proceedings of the ACS Rubber Division* Conference, Detroit, Michigan, 9 October.

Rogers, L. C., Johnson, C. D. and Keinholz, D. A. (1981). The modal strain energy finite element method and its application to damped laminated beams. *Shock Vibr. Bull.* **51.**

Soovere, J. and Drake, M. L. (1985). *Aerospace Structures Technology Damping Design Guide*. AFWAL-TR-84-3089.

Yui, Y. C. (1993). Finite element analysis of structures with classical viscoelastic materials. *Proceedings of the 34th Structures, Structural Dynamics, and Materials Conference*, La Jolla, California, April, pp. 2110–2119.